Results in Engineering 15 (2022) 100555

Contents lists available at ScienceDirect

Results in Engineering

journal homepage: www.sciencedirect.com/journal/results-in-engineering

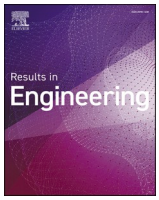

Reliability analysis-based investigation of the historical Széchenyi Chain Bridge deck system

Balázs Kövesdi [a], Dénes Kollár [a,*], László Dunai [a], Adrián Horváth [a,b]

[a] Budapest University of Technology and Economics, Faculty of Civil Engineering, Department of Structural Engineering, 3 Műegyetem rkp., Budapest, H-1111, Hungary
[b] Főmterv Co., Bridge Design Department, 37 Lövőház u., Budapest, H-1024, Hungary

ARTICLE INFO

Keywords:
Corrosion
Reliability analysis
Monte Carlo simulation
Damage assessment

ABSTRACT

Before the recent reconstruction, significant corrosion damages were observed on the deck system of the ~170-year-old Széchenyi Chain Bridge. Therefore, an advanced reliability analysis-based study is executed to assess the risk of failure of the structure in its situation until the refurbishment starts. The current paper has the aim to introduce the applied assessment method for the risk analysis and damage grade determination of the historical structure. The novel method combines the following techniques: (i) input data coming from on-site measurements implemented into state-of-the-art corrosion models, (ii) advanced finite element model-based resistance calculation (GMNI analysis) implemented into (iii) Monte Carlo simulation-based stochastic reliability assessment method to determine the risk of the bridge deck system failure. It is concluded that the introduced method is a powerful tool for risk assessment of existing aging structures.

1. Introduction and research aim

The Széchenyi Chain Bridge is a more than 170-year-old historical monument in Budapest, Hungary. The road bridge, with remarkable daily vehicular traffic, over River Danube is a major crossing between the two sides of Buda and Pest. Construction of the original structure started in 1839 and finished in 1849. It was considered as the largest chain bridge at that time with a maximum mid-span of 202.60 m (Fig. 1), while currently only the Hercílio Luz Bridge (339 m) in Brazil and Clifton Bridge (214 m) in England have larger spans. The original bridge, which was the first permanent bridge in the capital city, operated until 1914, because it had no stiffening girder and a lightweight timber deck system was used, and notable vibrations of the bridge deck were observed. Therefore, a new supporting structure was designed consisting of twenty-five carbon steel chain bars between each node with doubled length and increased load-bearing capacity compared to the previous structure; thus, distance between pins and suspension bars increased from 1.8 m to 3.6 m. The total mass of the ironwork increased to 5200 tons with the new truss stiffening girder using carbon steel with ultimate strength of 480–560 MPa, and a reinforced concrete deck was also constructed. The bridge was destroyed in 1945 during World War II. It was rebuilt without any significant changes of the structural system, and it was re-opened for traffic in 1949. Until 2019, no significant maintenance or reconstruction works had been made on the structure (except small corrosion protections), while chain elements have reached a lifetime of 100 years and the deck system is more than 70 years old. Several investigations and measurements had been carried out to assess corrosion conditions and structural behaviour (e.g., proof load tests in 2002 and 2018) and assist the renewal process (started in 2021) and design of the old bridge deck system. Cross-section of the bridge consisting of reinforced concrete slab and longitudinal steel stringers is shown in Fig. 2, which is the structural layout before the renewal process changing the reinforced concrete slab to steel orthotropic deck system.

The primary research aim of the current paper is the assessment of load-bearing capacity of the damaged and corroded bridge deck system and the determination of its risk of failure based on the corrosion conditions measured in 2019. On-site measurements and probabilistic analysis of the corroded chain elements were introduced by Kövesdi et al. [1] in 2017 leading to the conclusion the chain elements can safely carry their loads within their current corrosion state; however, maintenance of the corrosion protection of the bridge is urgent to ensure its safe operation.

Beside of the corrosion damages observed in the chain elements, significant damages were also observed in the bridge deck system, having remarkable material loss in the longitudinal steel beams under the concrete slab, especially near the expansion joints, where the water

* Corresponding author.
E-mail address: kollar.denes@emk.bme.hu (D. Kollár).

https://doi.org/10.1016/j.rineng.2022.100555
Received 12 May 2022; Received in revised form 13 July 2022; Accepted 19 July 2022
Available online 4 August 2022

could directly damage the structure. The current investigation is focusing on the load carrying capacity of the reinforced concrete slab and corrosion condition of steel parts (longitudinal stringers and cross-girders) of the bridge deck system. Results of previous measurements are taken into consideration in the reliability analysis, which is limited to the condition regarding 2019 and its load-bearing capacity. In the current paper, the applied assessment method for risk analysis is introduced. The applied method combines the following techniques: (i) corrosion models using on-site measurement results, (ii) advanced finite element model and analysis for resistance calculation (geometrically and materially nonlinear analysis with imperfections – GMNI analysis), and (iii) Monte Carlo simulation-based stochastic reliability assessment method.

At first, deterministic calculations are carried out to determine the load carrying capacity of the bridge deck using numerical simulations. In the next phase, stochastic analysis is performed using advanced corrosion model and Monte Carlo simulation technique with a confidence level corresponding to 1-year lifetime.

2. Research strategy

An extensive research strategy is developed in order to determine the reliability and the operational risk of the bridge deck system with high accuracy based on the corrosion measurement and condition survey conducted in 2019. The load carrying capacity of the bridge deck system and their design value is determined by two different theories using deterministic and stochastic design approaches. In both cases the ultimate resistance is determined by advanced numerical model using GMNI analysis, but the statistical assessment is applied differently. Within the numerical investigations different optional damage scenarios are analysed and the risk of failure is determined for the worst-case scenario leading to the lowest resistance and largest risk. Corrosion damage is taken into consideration with effective plate thickness in the deterministic calculations and characteristic resistance is calculated using GMNI analysis. Then, the design resistance value is determined using partial safety factors based on Eurocode design requirements.

In the stochastic analysis, parameters affecting the load bearing capacity such as geometrical dimensions and material properties are considered as probabilistic variables using first-order reliability method (FORM). Monte Carlo simulation is applied for determining the mean, characteristic and design resistances for each failure mode. Finally, finite element analysis-based probability density functions and cumulative distribution functions are used to evaluate the reliability index of the bridge deck and risk of failure. Resistance verification is carried out at two locations along the entire bridge including (i) a general segment, where the reinforced concrete deck and longitudinal stringers are continuous and (ii) in the vicinity of the expansion joints, which is the most critical region due to corrosion and longitudinal stringers are supported by corbels.

The applied approach for modelling corrosion deals with (i) separating local corrosion and global surface corrosion, (ii) differences between horizontal and vertical corroding surfaces, (iii) statistical parameters of non-uniform corrosion damages using the effective plate thickness method proposed by Kim et al. [2], (iv) corrosion depth (with maximum and mean value) and temporal change of its stochastic parameters by using the time-dependent empirical model of Paik and Kim [3], and (v) the change of mechanical properties over time due to corrosion (decrease of yielding plateau length and ultimate strain of structural steels), whilst characteristics of corrosion are different for structural steels and reinforcing rebars.

3. Literature review

A comprehensive literature study is carried out focusing on the determination of corrosion damage models, state variables, probabilistic variables and corrosion model parameters. One of the most common defects of existing bridges resulting eventually in severe failure is corrosion of steel elements. Numerous research deals with the cause of corrosion development, the temporal change of corrosion losses and their consideration in design. Therefore, the literature review is focusing on (i) the effect of corrosion on material properties, (ii) development of time-dependent, statistical-based corrosion models, (iii) consideration of corrosion losses in numerical models, and (iv) reliability analysis-based design of steel structures.

3.1. Corrosion

A number of laboratory tests shows that mechanical material properties of structural steel depend on the corrosion damage which can be explained by the local defects (notches) on corroded surfaces resulting in the origin of fracture on a lower loading level. It is well known that characteristics of stress-strain curves highly depend on the corrosion damage, the location, size and depth of dislocations [4]. According to Kim et al. [2], tensile tests show that yield strength and ultimate strength of structural steels are not significantly affected by corrosion if reduction of geometrical dimensions are taken into account. On the other hand, ultimate strain decreases nearly linearly with the increase of corrosion damage. In addition, several research [2,5] pointed out the disappearance of yielding plateau, or decrease in the length of yield plateau, in the case of severe degradation due to high corrosion damage. Fig. 3a demonstrates typical stress-strain curves taken from international literature for non-corroded and corroded structural steel tensile test specimens; corrosion damage ($\rho_{w=}A_{corr}/A_{total}$, where A_{corr} and A_{total} are corroded and total intact cross-sectional areas, respectively) is denoted for each curve. However, the same trend cannot be observed unambiguously for reinforcing steel rebars according to Ou et al. [6]. Ultimate strain decreased significantly in their tensile tests due to artificial corrosive environment, while natural corrosion did not have an unequivocal effect. Experimental results for naturally corroded reinforcing rebars are shown in Fig. 3b.

Corrosion is an extremely complex phenomenon, its formation and change over time are influenced by several geometrical, structural and environmental factors (e.g., humidity, temperature, exposure to salt water, etc.). There are several deterministic and stochastic-based corrosion models in the international literature for different steel materials as well as steel structures exposed to different corrosion effects. An advanced time-dependent empirical corrosion model for steel structures in marine environment was developed in 2012 by Paik and Kim [3]. The model was used and extended by Tohodi and Sharifi [7] for bridge structures in order to determine the load-carrying capacity of

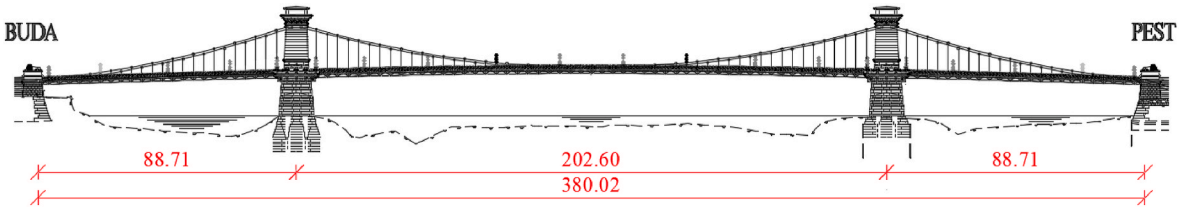

Fig. 1. Side view of the Széchenyi Chain Bridge, main dimensions [m].

locally corroded steel plate girder ends using artificial neural network. Fig. 4 shows the flow chart of the proposed corrosion model of Paik and Kim, and the time-dependent probabilistic characteristics of corrosion damage as well. The statistical scatter of corrosion damage and reduction of plate thickness due to corrosion at any exposure time can be analysed by the proposed method in a refined manner, using the following 3-parameter Weibull function (**Equation (1)**) to characterize the probability density distribution of the pit depth:

$$d_c(Y_e) = \frac{\alpha}{\beta}\left(\frac{Y_e}{\beta}\right)^{\alpha-1} \exp\left[-\left(\frac{Y_e}{\beta}\right)^{\alpha}\right] \quad (1)$$

where d_c is corrosion depth or pit depth, α is shape parameter, β is scale parameter, while Y_e is exposure time in years after the breakdown of the coating and can be calculated as $Y_e = Y - Y_c$, Y is the age of the steel structure or specimen, and Y_c is the corrosion protective coating life; the formula assumes that there is no corrosion damage until the end of coating life. On the other hand, the model includes the change of corrosion depth and its probability density over time and in the function of actual corrosion state.

Generally, the corrosion state can be modelled in finite element analyses by using two different approaches. Firstly, solid elements can be used in order to take the measured or hypothetical, corroded surface (using minimum, maximum and mean corrosion depth or roughness and corrosion models) into account by changing the nodal coordinates (i.e., upgrading the initial geometry configuration) of a flat surface based on imposed displacement constraints [8]. Basically, it is a possible modelling approach when a detailed surface measurement is available using three-dimensional scanning or roughness measurement with a maximum grid size of 1 mm. Similar approach was used to model the corroded chain elements of the studied bridge by Kövesdi et al. [1].

For realistic cases of structures under operating conditions when such measurements are not available, the corrosion state can be considered with an average reduction of plate thickness. Although the corrosion damage and roughness of constituent steel plates is non-uniform, and this could significantly affect the load bearing capacity. Therefore, Kim et al. [2] proposed to calculate the effective plate thickness t_{eff} based on laboratory experiments with $t_{eff} = t_{mean} - s$, where t_{mean} and s are mean plate thickness and standard deviation of the residual thickness, respectively which can be even implemented in finite element models using shell elements for large-scale structures. This approach provides a relatively simple approach to model corrosion and even though determine the strength of corroded steel elements with fair accuracy which is verified by laboratory experiments and tensile tests.

3.2. Reliability analysis-based design of steel structures

Annex C of EN 1990 [9], introducing the basis for partial factor design and reliability analysis, defines the measure of reliability for the failure mode considered within a corresponding reference period, i.e., design lifetime, by the survival probability $P_s = 1 - P_f$, where P_f is the failure probability in reliability analysis-based calculations (Level II and III in Fig. 5). The structure should be considered to be unsafe if P_f is larger than an appropriate prescribed target value P_0 since it does not fulfil the design criteria of the EN 1990. In the current paper, analysed structural members are verified by first order reliability method (FORM) using Monte Carlo simulation; therefore, background of these approaches is introduced hereunder in detail. The advanced design approach takes uncertainties of input variables into account based on statistical analysis and makes risk assessment of damaged structural elements possible. Generally, first order reliability methods (FORM) use an alternative measure of reliability, instead of applying failure probability directly, defined by the reliability index β. The relation between failure probability and reliability index is given in Table 1. Failure probability and fulfilment of design criteria can be represented with a performance function $g = R - E$, where R is resistance and E is effect of actions, while $P_f = \text{Prob}(g \leq 0)$ and g, R and E are probabilistic variables. The structure is adequate if $g > 0$, while $g < 0$ denotes failure. Reliability index can be calculated using $\beta = \mu_g/\sigma_g$ if g is a function with normal distribution, where μ_g and σ_g are the mean value and standard deviation of g, respectively. On the other hand, $P_s = 1 - P_f$ is recommended to use for the g performance function with non-normal distribution. Therefore, deviation of the density function from normal distribution in the calculation must be checked and the failure probability may be determined accordingly.

The target reliability index for ultimate limit state recommended by the standard for a reference period of 1 year (a lifetime of 1 year) is considered in the stochastic analysis, is $\beta_1 = 4.7$. This value includes the effect of uncertainties of loading and resistance in a combined way. In the present paper, only the resistance side is treated as a probabilistic variable in the calculation and loading is considered as a deterministic variable since probabilistic information on traffic loading was not available. The standard provides the possibility to separate the two sides at probabilistic level and therefore introduces the reliability index $\alpha_R \cdot \beta$

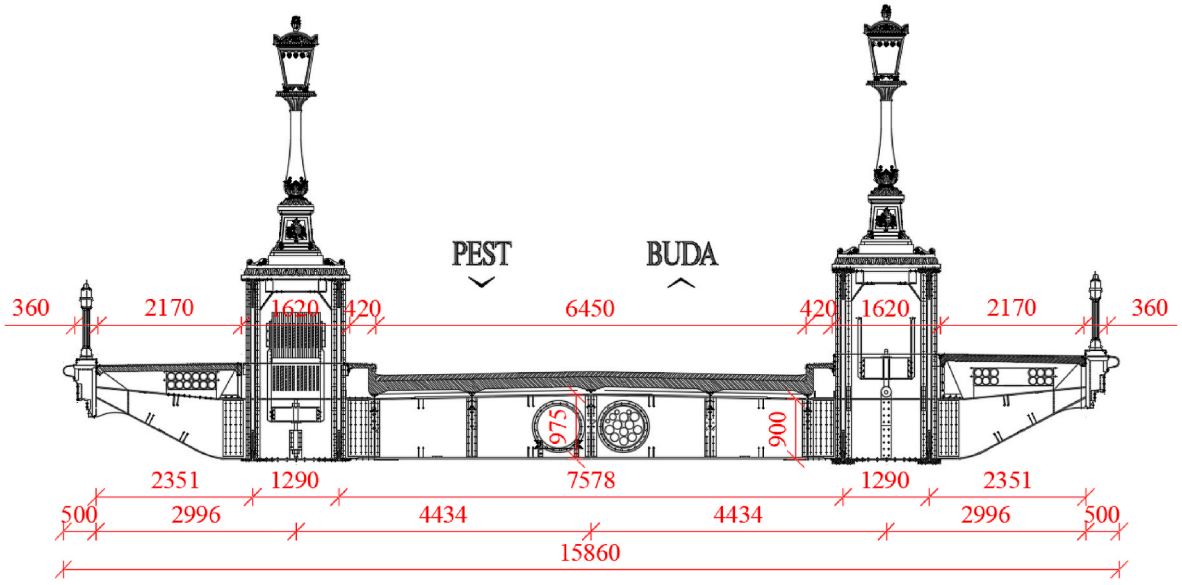

Fig. 2. Cross-section of the bridge before renewal, main dimensions [mm].

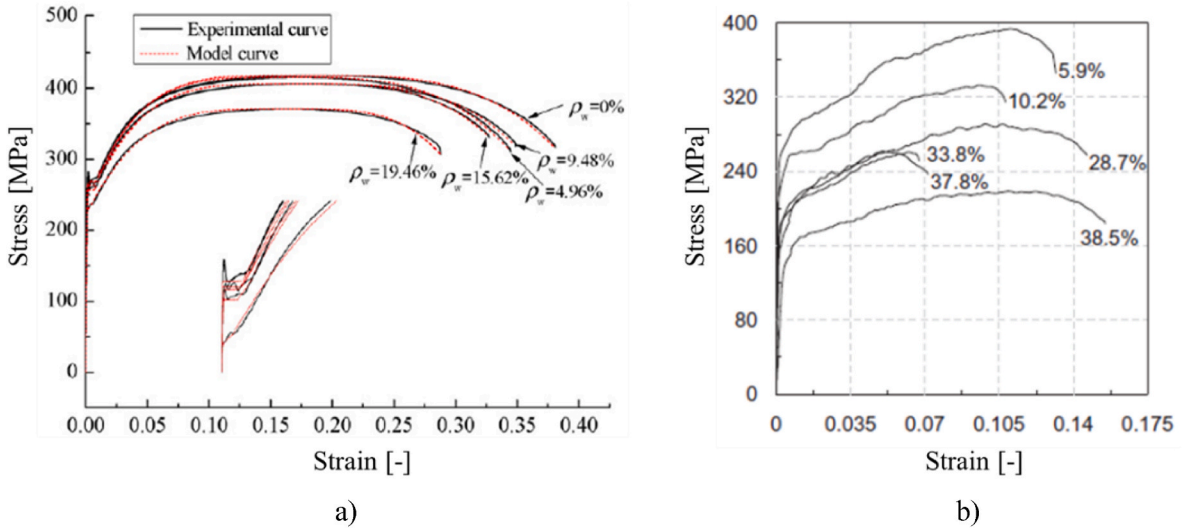

Fig. 3. Stress-strain curves of a) structural steel [5], and b) reinforcing steel rebars [6] for different corrosion damages.

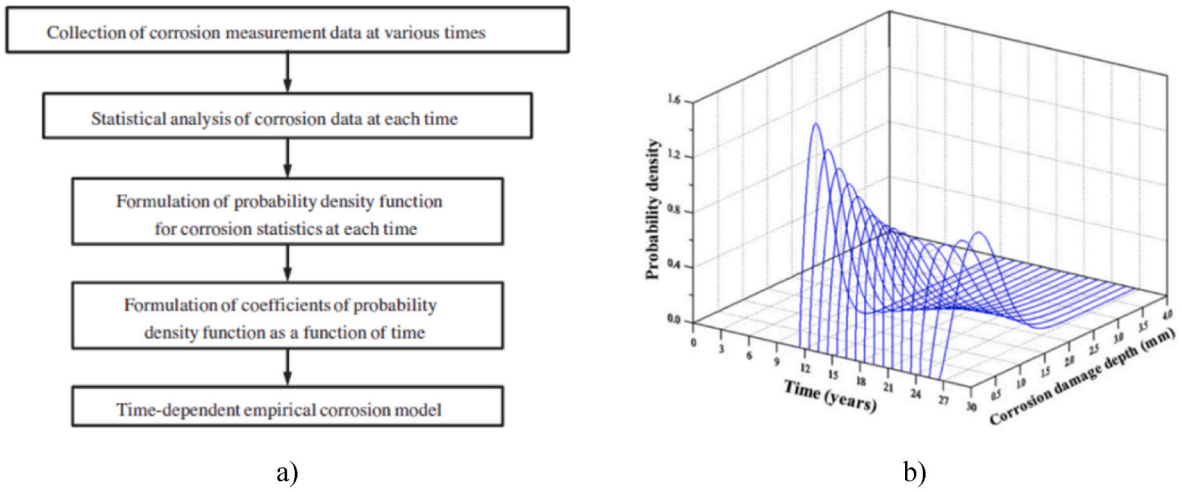

Fig. 4. a) Flow chart of the corrosion model of Paik and Kim [3], and b) time-dependent probabilistic characteristics of corrosion damage [3].

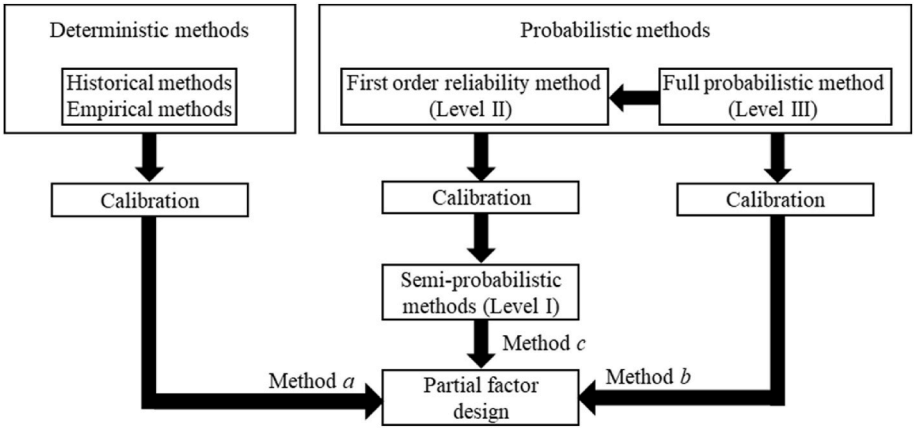

Fig. 5. Overview of reliability methods in EN 1990 [9].

(Fig. 6), which is used to determine the failure probability on the resistance side under deterministic loading using sensitivity factor $\alpha_R = 0.8$. Design point P and failure boundary (S), where $g = R - E = 0$, are also shown in Fig. 6.

Actual values of probabilistic variables are determined using Latin hypercube sampling method in order to perform Monte Carlo simulation. This method differs from the traditional random sampling procedure [10] since it avoids the grouping of selected values during

Table 1
Relation between failure probability P_f and reliability index β based on EN 1990 [9].

P_f	10^{-1}	10^{-2}	10^{-3}	10^{-4}	10^{-5}	10^{-6}	10^{-7}
β	1.28	2.32	3.09	3.72	4.27	4.75	5.20

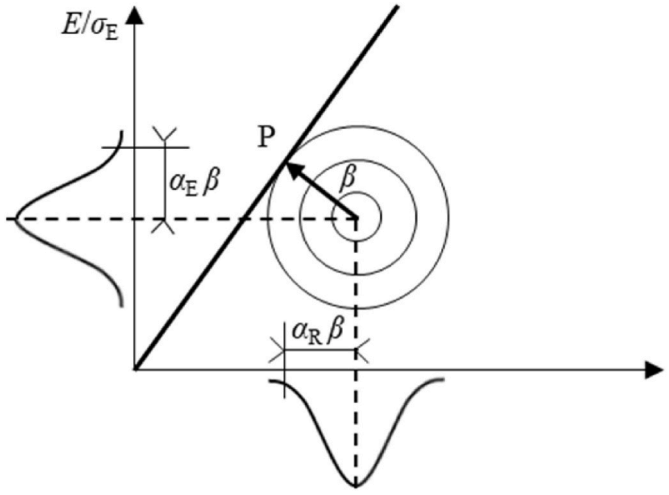

Fig. 6. Design point P and reliability index β according to the first order reliability method for uncorrelated variables with normal distribution based on EN 1990 [9].

random generation. By completely random sampling, some ranges may be left blank, and in other ranges, the points may be close to each other, as shown in Fig. 7. Another advantage of the Latin hypercube sampling technique is that it also selects from low probability values at the limit of distribution, which is important in determining the characteristic (5%) and design (1‰) resistance values. The number of samples (n) required for the Monte Carlo simulation does not depend on the number of probabilistic variables but on the desired probability. For a reliable evaluation of the low probability ranges, a sample of $n \approx 30/P$ to $100/P$ is required, where P is the desired probability.

Thus, number of samples is $n \approx$ 600–2000 for the characteristic resistance ($P = 5\%$) and $n \approx 30{,}000 \div 100{,}000$ samples are justified for a reliable result for the design resistance ($P = 1‰$). One possible solution for reducing samples is the application of the response surface methodology. In this case, a response surface is fitted to the results obtained during the Monte Carlo simulation using quadratic regression model. However, the number of samples required for the proper fit of the response surface during the first Monte Carlo simulation depends on the number of probabilistic variables.

4. On-site measurements

During the preparation of reconstruction plans by the consortium of Főmterv Co, MSc Ltd. and CÉH Ltd, the following information was available about the corrosion state of the bridge deck:

- Significant damage can be seen under the deck, mainly in the elements near the curb, and in the span near Buda there are also damages from vehicle collisions.
- Strengthening of cross beams was required during the previous reconstruction (between 1987 and 1988). Damage due to soaking is mainly visible at the curb.
- Severe corrosion damage can be seen on the two outer longitudinal stringers (out of five longitudinal stringers) as a result of soaking under the curb. The corrosion protective coating system of the steel structure was destructed on the bridge.
- Steel curbs on the outer sides of pedestrian sidewalks are severely damaged.
- The reinforced concrete deck was built after the Second World War and was not changed during the reconstruction in 1987–1988. Due to soaking of the insulation, the edge bands of the deck were severely damaged, and the chloride ion content was measured to be very high.
- Water was leaking through expansion joints.

Since the present study focuses on the bridge deck, therefore solely the corrosion state of the longitudinal stringers, cross beams and reinforced concrete deck is described in this section. Measurement data based on the condition survey carried out in November 2019 serve as input for the static calculations and reliability analysis presented in the following sections.

Extraction of concrete samples from the reinforced concrete slab was carried out at five locations to determine the strength characteristics of concrete and the corrosion grade of the reinforcing rebars. Following conclusions were drawn based on the investigation. Firstly, top reinforcement was undamaged at all the five sampling locations and plain

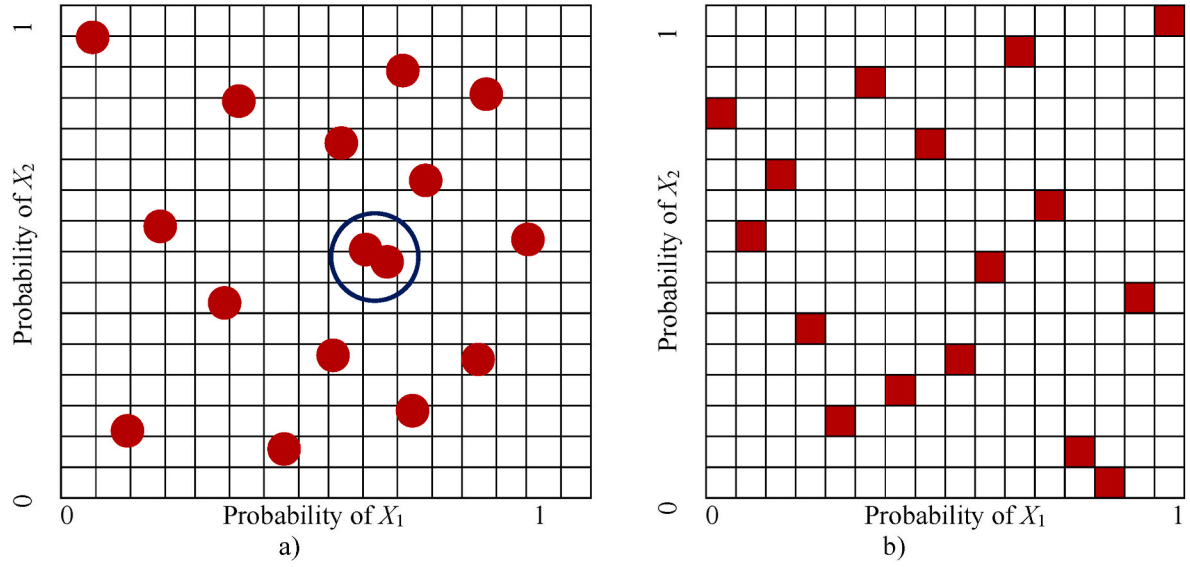

Fig. 7. Random (left) and Latin hypercube (right) sampling methods.

reinforcing rebars are used with average diameter of 8 mm in the longitudinal direction. Bottom reinforcement was corroded, concrete cover detached due to the evolving rust in several places (Fig. 8a and **b**). Spacing and location of reinforcement is not uniform in the examined locations, it varies along the length of the bridge, while the disorder of reinforcing rebars can be observed in several places, as shown in Fig. 8c. The concrete cover of top reinforcement is uniformly 4–5 cm, which is significantly larger than the 2 cm assumed in the static calculation of the time. Transverse reinforcement spacing is 7.5 cm at two tested locations and 10 cm based on the other three sample locations, while the spacing of longitudinal rebars is typically between 4 and 5 cm. Chloride content of drilled dust samples in all cases exceeded the limit value of 0.4 m% by 3–11 times. Thus, the concrete slab is heavily contaminated with chloride ion, which may result from the increase of salt concentration due to frequent drying after soaking, or from salt vapour engaging unprotected concrete surfaces. Concrete of the slab is very porous with low density (average value of 2212 kg/m^3). The mean compressive strength is 30.8 MPa, which corresponds to the concrete quality of C16/20 according to the currently valid MSZ 4798:2016 Hungarian standard.

The corrosion conditions and corrosion state of steel elements were examined, and the following conclusions were drawn based on the pointwise measurements. The corrosion state of outer longitudinal stringers was critical, since locally, in the vicinity of the joint of stringer and cross beam by the expansion joint the average corrosion damage depths (or corrosion waste, i.e., reduction of thickness) was 80% in the web (Fig. 9a), although the web was perforated in few locations, while a section loss of ~20% could be measured in the lower and upper flanges in several places (Fig. 9b). In addition, there were local corrosion defects covering a smaller area with a corrosion waste of 5–10% at many places (Fig. 9c). The inner three longitudinal stringers were in a condition corresponding to the age, without significant corrosion damage (Fig. 9d).

5. Numerical model development

A numerical model is developed in ANSYS, a general-purpose finite element program in order to investigate the influence of corrosion on structural performance and reliability of the deck plate by using first-order reliability method (FORM) and performing geometrically and materially nonlinear analysis with imperfections. Large deflection effects are included in the static analysis, while stress stiffening effects are automatically included in all geometrically nonlinear analyses in the program. Sparse solver is used with full Newton-Raphson method updating the stiffness matrix at each equilibrium iteration. In addition, line search option is activated to improve the efficiency of the iterative method. Automatic time stepping is turned on to control incremental force-controlled loading. A combined finite element model is developed using beam, shell and solid elements. A segment of the bridge with a length of ~11.5 m is modelled containing four cross beams. Steel truss stiffening girders, chain elements, suspension bars, the wind bracing system and reinforcing rebars are modelled using linear two-node beam elements (BEAM188). The finite element type is based on Timoshenko beam theory including shear deformation effects and permits unrestrained warping of cross-sections. Steel cross beams and longitudinal stringers are modelled using linear four-node shell elements (SHELL181) using reduced integration scheme. The finite element type is based on first-order shear deformation theory (Mindlin-Reissner shell theory). Low-order eight-node hexahedral elements (SOLID185) with enhanced strain element technology and pure displacement formulation are applied in the reinforced concrete deck. Multilinear kinematic hardening models are used for steel, concrete and reinforcing rebars (schematic representation in Fig. 10) in the numerical simulations using von Mises yield criterion and associative flow rule.

Different material properties are used in deterministic and stochastic analyses. All material properties are set to characteristic values in

Fig. 8. a-b) Corrosion of bottom reinforcement and detachment of concrete cover due to rust and c) disorder of reinforcing rebars (Source: Provix Híd Ltd.).

Fig. 9. Corrosion state of a) outer longitudinal stringer near the expansion joint, b) lower flange of outer longitudinal stringer, c) smaller areas with local corrosion defects and d) inner longitudinal stringers (Source: Provix Híd Ltd.).

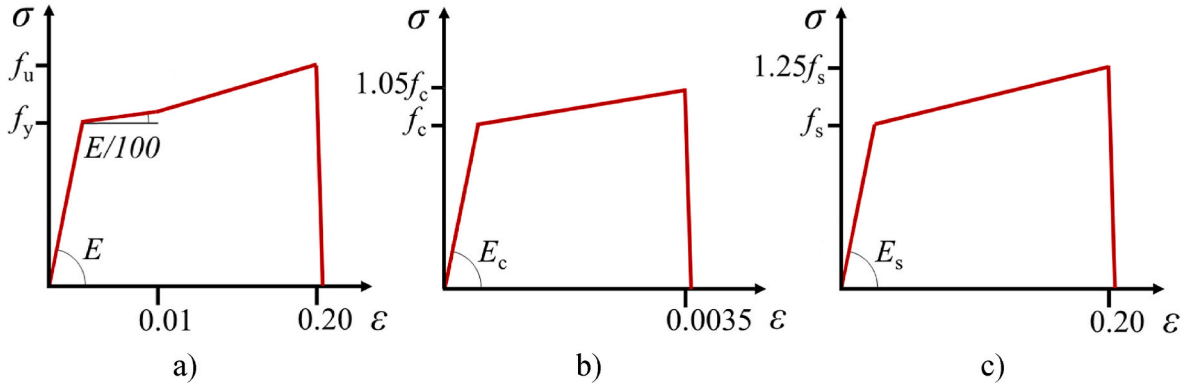

Fig. 10. Applied material models for a) steel, b) concrete and c) reinforcing rebars.

deterministic calculations, while properties are considered probabilistic variables in probability analysis. Yield strength for structural steel and compressive strength for concrete are taken into account with the corresponding mean values and standard deviations. The recommendation of Joint Committee on Structural Safety (JCSS) is applied for the probability distribution of structural steel and reinforcing rebars by setting the mean yield strength as an increased nominal value (f_{nom}) by 14%, while the coefficient of variation (ν) is 0.07. Normal distributions are assumed for the material properties with the following input data:

- longitudinal stringers, cross beams, truss stiffening girders, chain elements, suspension bars and wind bracing system (structural steel S235)

  Note: Yield strength f_{yk} = 235 MPa is used in deterministic calculations, while mean value $f_{ym} = 1.14 \cdot f_{yk}$ and coefficient of variation $\nu_{fy} = 0.07$ are applied in stochastic analysis.

- reinforcing rebars (steel grade B240B equivalent to steel grade 36.24)

  Note: No measurements were performed, while steel grade was not indicated in the original calculations. The documentation from 1948 denotes permissible stress equal to 140 MPa for rebars, which is approximately identical to 144 MPa for steel grade B240B recommended in Hungarian standard ÚT 2–3.414. Yield strength $f_{sk} = 240$ MPa is used in deterministic calculations, while mean value $f_{sm} = 1.14 \cdot f_{sk}$ and coefficient of variation $\nu_{fs} = 0.07$ are implemented for stochastic analysis.

- concrete slab (C16/20)

Note: Concrete compression tests give a mean compressive strength $f_{cm} = 30.8$ MPa and coefficient of variation $\nu_c = 0.16$, used in stochastic analysis, yielding characteristic value $f_{ck} = 30.8$ MPa–8 MPa = 22.8 MPa according to EN 1992-1-1 [11]. However, characteristic compressive strength $f_{ck} = 16$ MPa based on concrete strength classes of the standard is used in deterministic calculations.

Locations and the extent of corrosion are taken into consideration in the numerical model based on on-site measurements and general corrosion assessment of the bridge. The following average (mean) corrosion damage depths (or corrosion waste, i.e., reduction of thickness) are taken into account for steel parts in the finite element model:

- upper and lower flanges of outer longitudinal stringers in general: 50%,
- web of outer longitudinal stringers in general: 30%,
- web, upper and lower flanges of inner longitudinal stringers in general: 10%,
- upper and lower flanges of outer longitudinal stringers near the expansion joint: 50%,
- web of outer longitudinal stringers near the expansion joint: 80%,
- web of outer longitudinal stringers aside the stiffener above the corbel (near the expansion joint): 80%,
- reinforcing rebars at the bottom of the slab: 30%.

The given values are considered in the initial configuration for deterministic analysis, while in the stochastic analysis these are the mean values in the corresponding probability density functions.

Two typical cross-sections are investigated: i) longitudinal stringers near the expansion joint and ii) internal longitudinal stringers. Longitudinal stringers are supported by corbels, while upper flanges are continuous above the cross beams. Location and rebar spacing of longitudinal and transverse reinforcing rebars are modelled based on on-site measurements as original reinforcement construction drawings did not remain. Isometric and cross-sectional views of the submodel are shown in Figs. 11 and 12, respectively. Each end section of the model is constrained in order to represent the boundary conditions of the submodel. Joints between the slab and steel flanges are modelled by defining sets of coupled degrees of freedom in vertical and transverse directions. A mesh sensitivity analysis was carried out to verify the finite element model. Based on the model verification, the average applied element size is 400 mm; however, longitudinal stringers have a finer mesh using shell elements with an average size of 70 mm. The numerical model contains 12,500 finite elements and 14,400 nodes.

Design of the reinforced concrete slab in ultimate limit state is based on analytical calculations as height of the compression zone is precalculated in the analysed cases assuming tensile strength of the concrete can be ignored. Thus, finite elements in the tensile zones representing concrete material are inactivated. An algorithm is developed to determine the extension of cracking in all the load cases and rebuild the slab based on analysed location and material properties. Thickness of the slab is decreased by 20 mm–130 mm (plus the haunch has a height of 20 mm above the longitudinal stringers) since lower concrete cover is practically missing, while upper reinforcing rebars are trampled down in the majority of the cases resulting in a concrete cover of 40–50 mm. The modelling concept of reinforced concrete slab in the outer span is shown in Fig. 13 assuming that the outermost longitudinal stringer does not resist any load due to a severe corrosion state. It may seem to be a rough assumption, but on-site measurements highlighted that it could be a possible scenario.

Permanent loads (self-weight and an asphalt layer with a thickness of 9 cm) and the permitted traffic loads are considered in the numerical investigation. Traffic load model of European standard EN 1991–2 is not used in the static verification since traffic is limited on the bridge due to the demonstrated circumstances. Thus, load model 'C' (Fig. 14) according to Hungarian standard ÚT 2–3.401 is applied with axle loads of 66.6 kN and 133.3 kN (distribution of forces in the asphalt layer is taken into account with an angle of 45°). Axle loads are multiplied by a dynamic amplification factor of 1.4 determined for the deck system. Note that the new orthotropic bridge deck has been designed considering predefined bus types crossing the bridge daily with maximum axle load of 125 kN, which is smaller than 133.3 kN; therefore, the current static verification is on the safe side regarding traffic loading.

Two load cases are analysed for both investigated parts (longitudinal stringers near the expansion joint and internal longitudinal stringers). Both locations of maximum positive bending moment and maximum shear force of the longitudinal stringer are analysed. In addition, maximum positive bending and punching of the slab are also investigated. Thus, five load cases are evaluated in the numerical calculations and approximate structural resistances are assessed based on deterministic analyses. On the other hand, reliability index is evaluated for the most hazardous load case using stochastic analysis. Fundamental combination of actions for persistent or transient design situations is used in both deterministic and stochastic analyses according to EN 1990 (Section 6.4.3.2, equation 6.10). Partial safety factors are $\gamma_G = 1.35$ for permanent loads and $\gamma_Q = 1.35$ for traffic load. The five load cases are as follows based on the position of concentrated traffic load (Figs. 15 and 16):

a) Load case 1 (LC1): stringer beside the expansion joint, maximum positive bending moment,
b) Load case 2 (LC2): vicinity of the expansion joint, maximum shear force,
c) Load case 3 (LC3): internal stringer, maximum positive bending moment,
d) Load case 4 (LC4): internal stringer, maximum shear force,

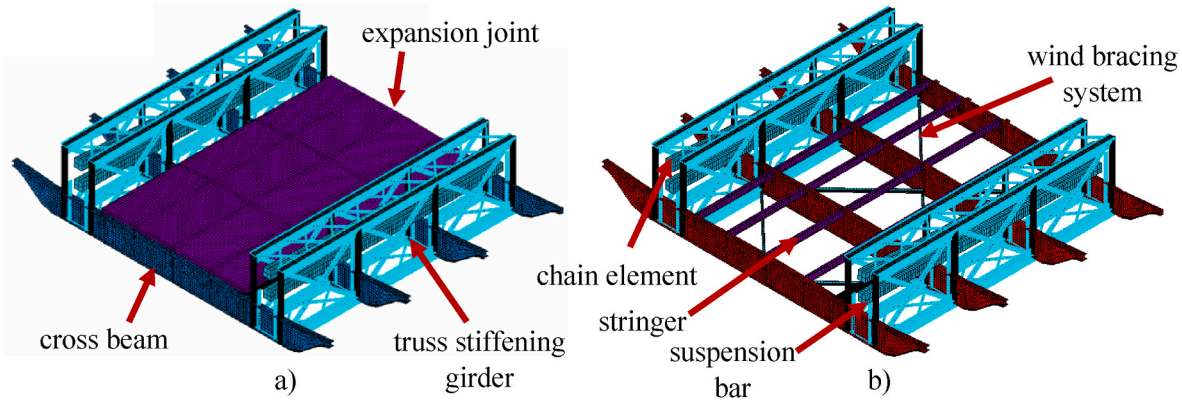

Fig. 11. Isometric view of the finite element model a) with and b) without reinforced concrete slab.

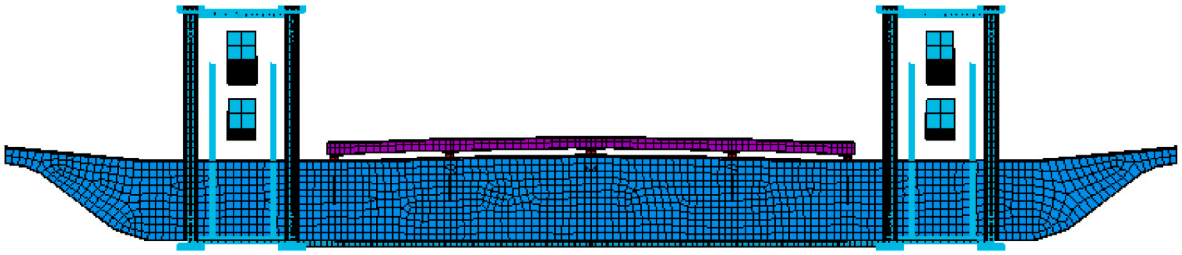

Fig. 12. Cross-sectional view of the finite element model.

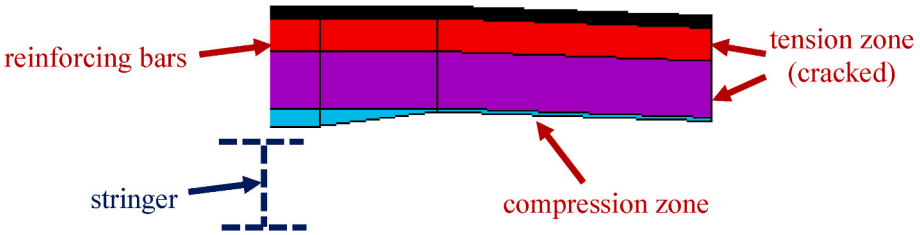

Fig. 13. Modelling concept of reinforced concrete slab in the outer span.

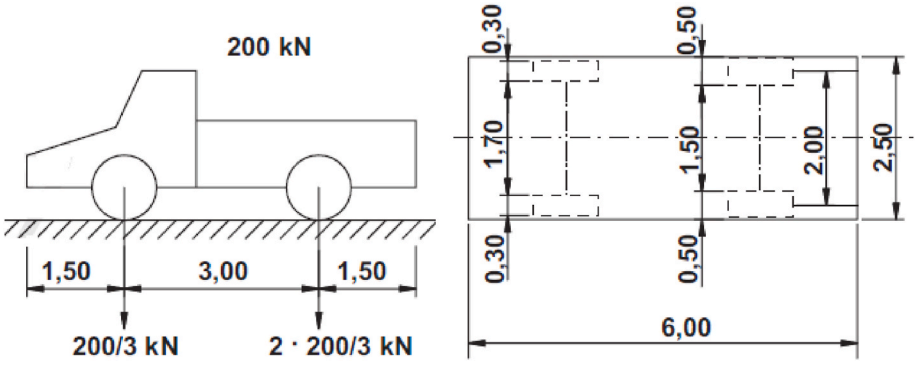

Fig. 14. Traffic load model 'C' according to Hungarian standard ÚT 2–3.401 [12].

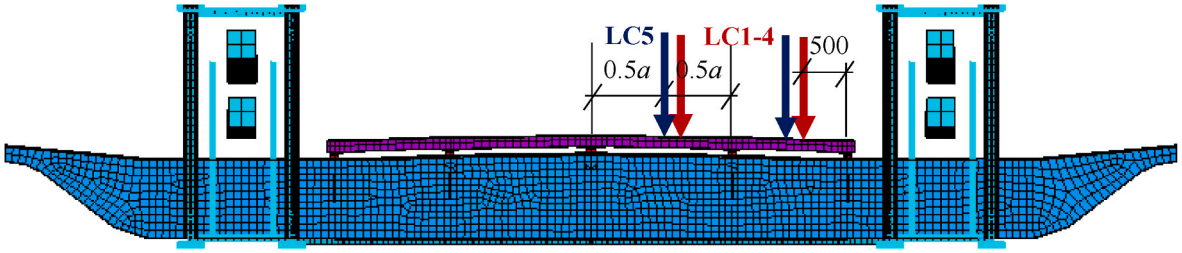

Fig. 15. Traffic load position in transverse direction.

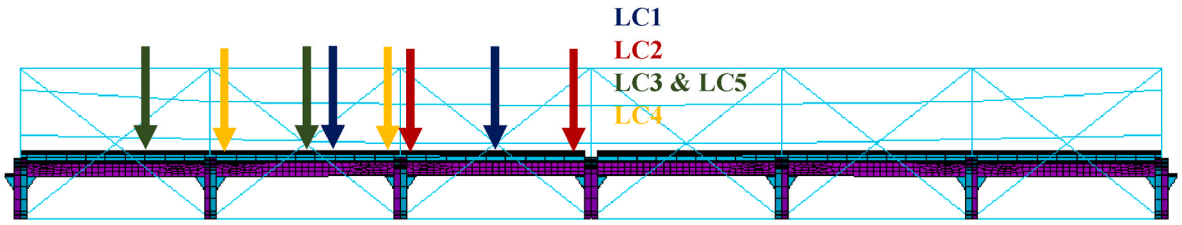

Fig. 16. Traffic load position in longitudinal direction.

e) Load case 5 (LC5): similar to LC3, but traffic loads induce maximum bending moment in the slab in transverse direction.

Equivalent geometric imperfections are included in the models in order to determine the load carrying capacity of the analysed structure. Imperfections are defined based on the appropriate eigenshapes of the structure representing local and global buckling modes using linear bifurcation (eigenvalue) analysis. The magnitudes of applied imperfections have recommended values in EN 1993-1-5 Annex C [13]. Equivalent geometric imperfections consider initial geometric imperfections of members as governed by geometrical tolerances, structural imperfections due to manufacturing and erection, residual stresses, and the variation of yield strength according to EN 1993-1-1 [14]. Different eigenshapes are used depending on the dominant failure mode for each load case (Fig. 17). Plate buckling mode (Fig. 17a) is scaled in case of maximum positive bending moment (LS1, LS3 & LS5), while shear buckling mode (Fig. 17b) is used in case of maximum shear force (LS2 & LS4). Local out-of-plane imperfections with a magnitude of $h_w/200$, where h_w is the web height, are defined in both cases.

Within the analysis three different failure scenarios are examined as follows:

- the reinforced concrete deck has an adequate strength to resist the loads, the failure of longitudinal stringers and cross beams are analysed and assessed based on the corrosion state surveyed in 2019,
- the failure of corroded reinforced concrete deck with defects is analysed based on the condition survey, while steel elements can resist loads without any failure,
- the failure of corroded reinforced concrete deck and mostly corroded steel members (near the expansion joint) is analysed simultaneously analysing whether substantially corroded longitudinal stringers fail to resist loading and what would be the reliability of the reinforced concrete deck to resist loads.

Definition of failure scenarios and separation of the damage within the concrete and the steel elements were necessary to be able to separately evaluate the risk of the analysed critical structural members. In the present paper only the third scenario is presented in detail, making the optional combined failure of the concrete slab and steel stringers possible.

6. Results of deterministic numerical calculations

First, deterministic analyses are carried out before performing stochastic analysis in order to determine the most hazardous load case. Two analysis types are included in deterministic numerical calculations: i) geometrically and materially nonlinear analysis with imperfections (GMNI analysis) for the determination of load carrying capacity as it is introduced in the previous section, and ii) geometrically nonlinear analysis with imperfections (GNI analysis) neglecting material nonlinearities in order to evaluate where elastic and plastic structural behaviours come apart and to assess load factors designating the presence of first yield in the modelled bridge segment. The presented results for the two most relevant load cases (LC2 & 5) focus on the introduction and evaluation of load factor based on force-vertical displacement curves and failure mechanisms. One node of the analysed longitudinal stringer below the rear axle is selected for comparison purposes. Calculated vertical displacements of the upper flange are evaluated. Load factors are denoted in the vertical axis representing the scaling factor for permanent loads and the applied traffic load model. A load factor of 1.0 means the fundamental combination of actions for persistent or transient design situations including partial safety factors and the dynamic amplification factor.

The vicinity of the expansion joint is analysed in load case 2 (LC2), where the rear axle of the traffic load model above the corbel of the stringer represents the loading situation for maximum shear force. The load factor-displacement curves and the difference of GMNI and GNI analyses are presented in Fig. 18. The failure mechanism is shown in Fig. 19 showing increasing load factors, out-of-plane displacements, and von Mises stresses. Curves come apart with load factor $\alpha = 0.55$ due to shear buckling of stringer web (Fig. 19b) and first yield (Fig. 19c). The characteristic load factor $\alpha = 1.05$ denotes the characteristic resistance in conjunction with partial factor $\gamma_{M1} = 1.10$ for stability resistance of shear buckling according to EN 1993-1-5 [13], resulting in utilization $\eta = 105\%$.

The rear axle of the traffic load model is positioned in longitudinal and transverse directions in order to analyse the maximum positive bending moment of the reinforced concrete slab in load case 5 (LC5). Load factor-displacement curves and the difference of GMNI and GNI analysis are presented in Fig. 20. The failure mechanism is presented in Fig. 21 showing increasing load factors, von Mises stresses and strains. Curves come apart with load factor $\alpha = 1.01$ due to first yield (Fig. 21a). Nevertheless, it does not mean the failure of the entire structure. Hardening and redistribution of moments (reinforced concrete slab resists increased load instead of longitudinal stringer after yielding) result in further load increments. Failure of the concrete slab (Fig. 21b), between the second and third stringer in transverse direction, by reaching the ultimate compressive strain ($\varepsilon_{cu} = 0.35$ %) occurs at load factor $\alpha = 2.09$.

On one hand, sufficient resistance of the analysed concrete deck is proved in accordance with on-site measurements and traffic limitations on the historical Széchenyi Chain Bridge, however, the stringers show

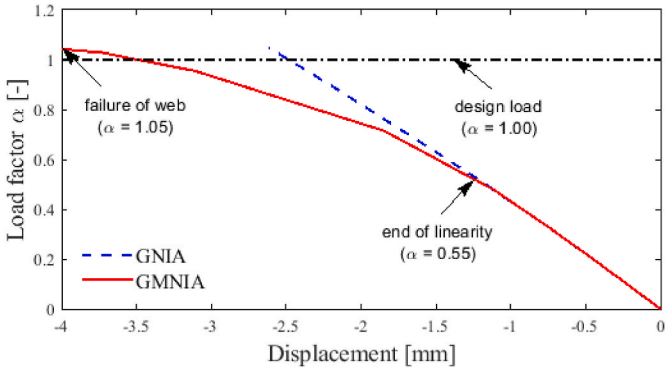

Fig. 18. Load factor-displacement curves, LC2.

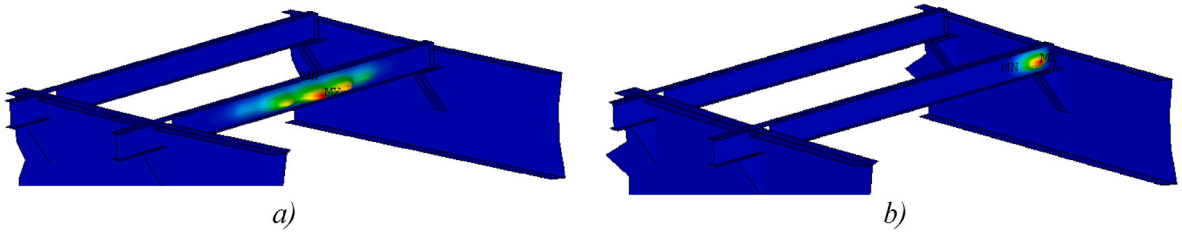

Fig. 17. Eigenshapes based on bifurcation analysis: a) plate buckling due to bending stresses and b) shear buckling.

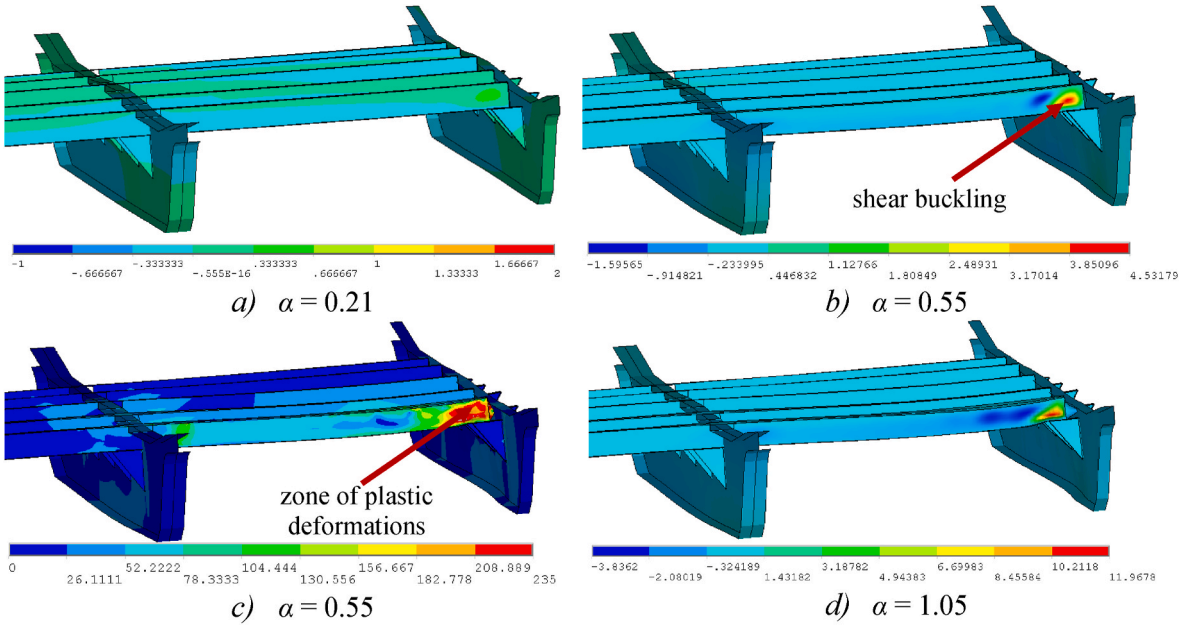

Fig. 19. Failure mechanism, LC2, a, b, d) out-of-plane displacement Ux [mm] and c) von Mises stresses [MPa].

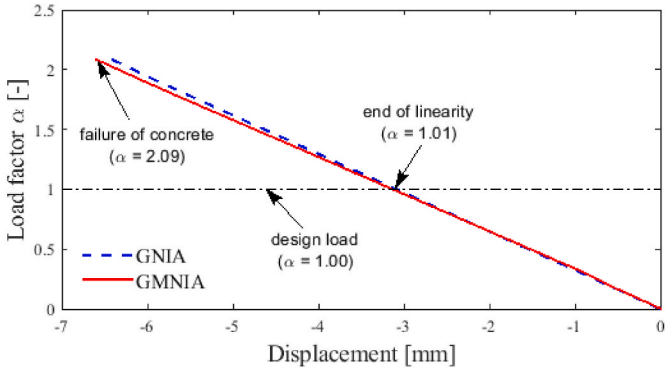

Fig. 20. Load factor-displacement curves, LC5.

5% overloading. It should be noted that deterministic calculations do not consider uncertainties in corrosion damage depth and thus the effect on reliability. Average corrosion damage depths based on on-site measurements are applied in latter calculations; however, corrosion waste can be both more or less resulting in severe or slight reduction of plate thickness. Therefore, the risk assessment analysis of the deck is carried out using stochastic finite element analysis, which is introduced in the next section.

7. Results of stochastic numerical simulations

7.1. Input data of the simulation

A total of five probabilistic variables are used in the stochastic analysis, the parameters are summarized in Table 2, where t_w and t_f are web and flange effective thickness, respectively.

Examples for probability density functions of remaining thickness of corroded plates considered in the model are shown in Fig. 22. The effect of surface roughness and non-uniformity within the plates is considered using the effective plate thickness approach. Actual values of probabilistic variables are determined using a Latin hypercube sampling method in order to perform Monte Carlo simulation.

In this case, a total of at least $n = 32$ virtual experiments are required for 5 variables. Therefore, $n_1 = 32$ samples are used for the Monte Carlo simulation performed in the first step. Afterwards, another Monte Carlo simulation is applied to the fitted response surface, where random sampling is also performed based on the given distributions. However, load bearing capacities in this case are not determined by new analyses but by using the approximation function generated for the response surface. In this second simulation step, $n_2 = 100{,}000$ is used, which meets the requirements given above for minimum sampling number.

7.2. Simulation results and risk assessment analysis

Deterministic calculations showed the most hazardous load case is LC2, where the vicinity of the expansion joint is analysed and the rear axle of the traffic load model, above the corbel of the stringer, represents the loading situation for maximum shear force. Therefore, the stochastic analysis is also carried out focusing on this load case and the corresponding failure mode (shear buckling of stringer web). Probability density function of simulated load factor α based on Monte Carlo simulation is shown in Fig. 23 in accordance with fitted probability density functions, while corresponding distribution functions are shown in Fig. 24. Characteristic load factors are also shown in the figure by intersecting cumulative distribution functions with a constant line representing $P_f = 5\%$. A relatively large coefficient of variation is evaluated, which is a result of the corrosion model and high level of uncertainty associated with corrosion damage depth. Four types of probability distributions are fitted to numerical data in order to (i) verify whether assumption of using formulae for the reliability index in EN 1990 for normally distributed data can be applied, and (ii) determine which probabilistic variable governs the failure. The following probability distributions are used in the comparison (parameters describing each distribution, which are denoted in Fig. 23, are also listed):

- normal (Gaussian): mean μ, standard deviation σ,
- lognormal: mean of logarithmic values μ, standard deviation of logarithmic values σ,
- Weibull (type III extreme value distribution): scale parameter α, shape parameter β,
- Gumbel (type I extreme value distribution): location parameter μ, scale parameter σ.

Fitted probability density functions and cumulative distribution

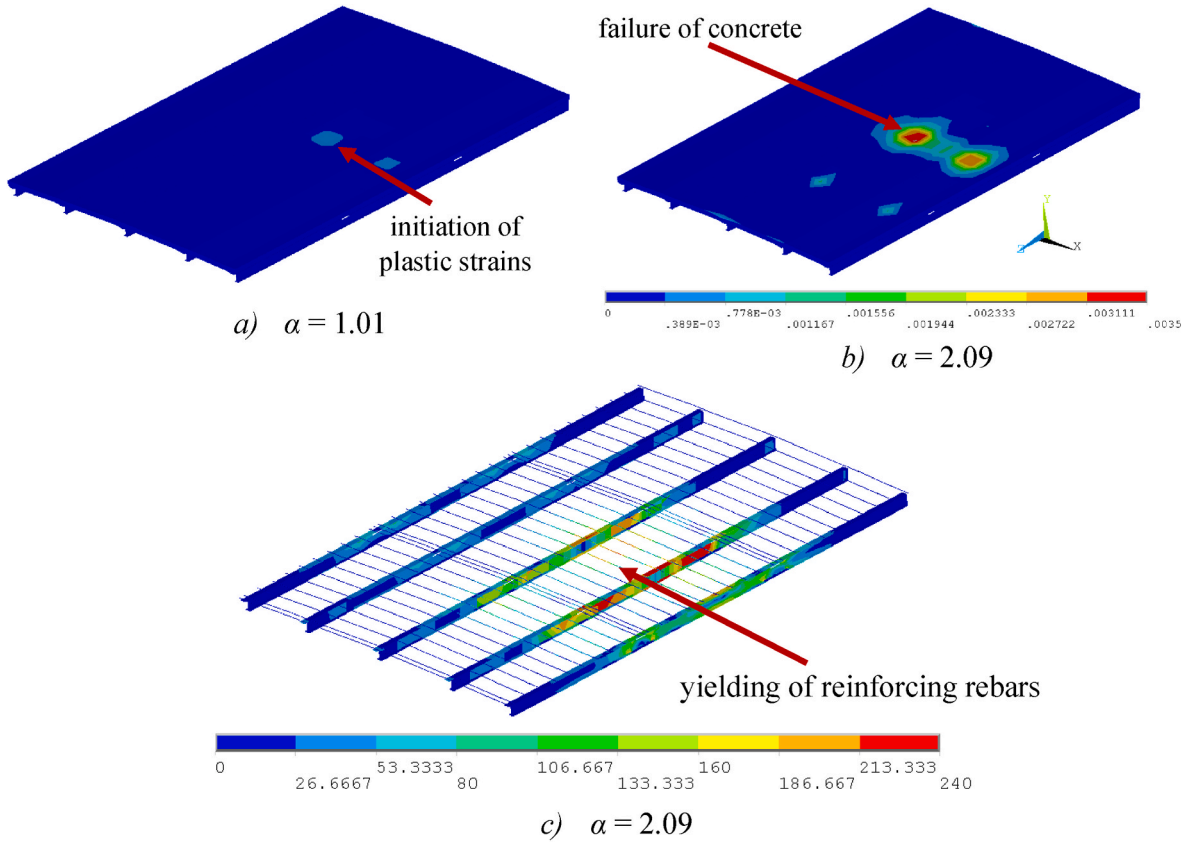

Fig. 21. Failure mechanism, LC5, a-b) von Mises plastic strains [−] and c) von Mises stresses in reinforcing rebars and longitudinal stringers [MPa].

Table 2
Applied probabilistic variables and stochastic parameters.

Variable		Distribution	Mean value	Additional parameters
Yield strength of structural steel	f_y	Normal	268 MPa	$\nu_{fy} = 0.07$
Compressive strength of concrete	σ_c	Normal	30.8 MPa	$\nu_c = 0.16$
Yield strength of reinforcing rebar	f_s	Normal	274 MPa	$\nu_{fs} = 0.07$
Corrosion damage of longitudinal stringer web	$d_{c,w}$	Weibull	80% near expansion joint 30% in general cases	$\alpha = 10$; $\beta = 0.2 \cdot t_w$ $\alpha = 10$; $\beta = 0.7 \cdot t_w$
Corrosion damage of longitudinal stringer flange	$d_{c,f}$	Weibull	50% near expansion joint 50% in general cases	$\alpha = 10$; $\beta = 0.5 \cdot t_f$ $\alpha = 10$; $\beta = 0.5 \cdot t_f$

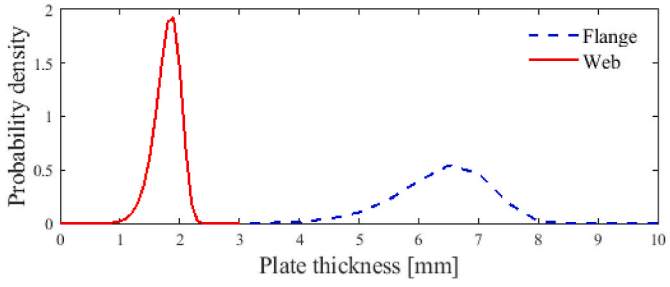

Fig. 22. Weibull probability density functions for flange (α = 10, β = 0.5·13.5 mm) and web near the expansion joint (α = 10, β = 0.2·9.4 mm).

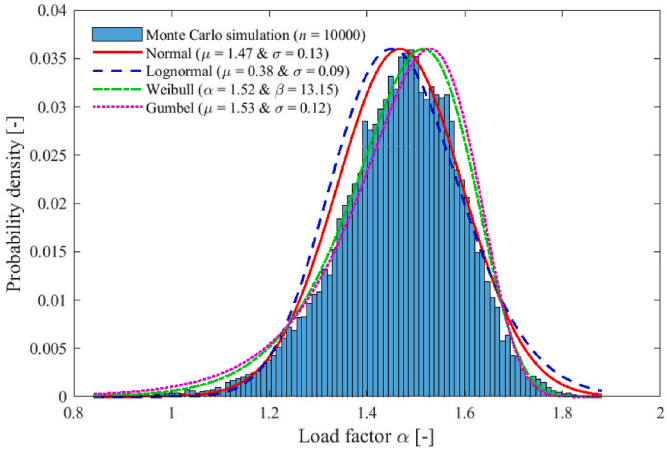

Fig. 23. Monte Carlo simulation-based and fitted probability density functions of load factor α.

functions show extreme value distributions, Weibull and Gumbel, are capable of describing the realistic behaviour. However, quantile-quantile plots (q-q plots) are added (Fig. 25) to visualise and assess whether Monte Carlo simulation-based sample data comes from a specified distribution. If the distribution of the sample data is in accordance with the specified distribution, the plot appears linear (shown with red dashed line). Based on Fig. 25c, Weibull distribution is the best choice for tracking the phenomenon of shear buckling of the corroded web plate. It is in agreement with the design formula in EN 1993-1-5 which depends on the cross-sectional area of the web and the slenderness of the analysed plate. Both parameters include the corrosion damage, which is considered by Weibull distribution. On the other hand,

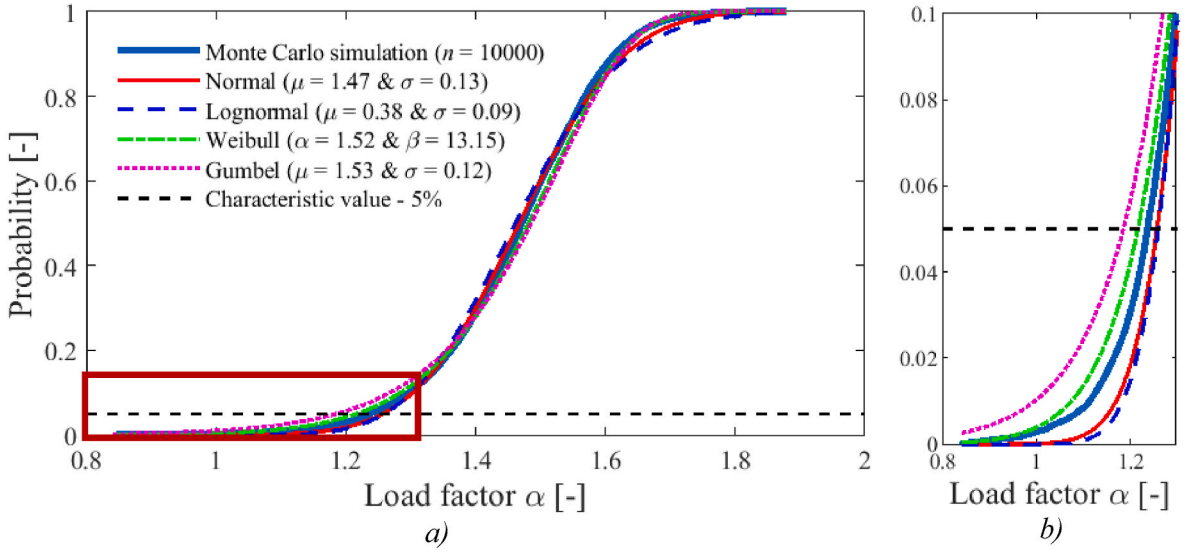

Fig. 24. Monte Carlo simulation-based and fitted cumulative distribution functions.

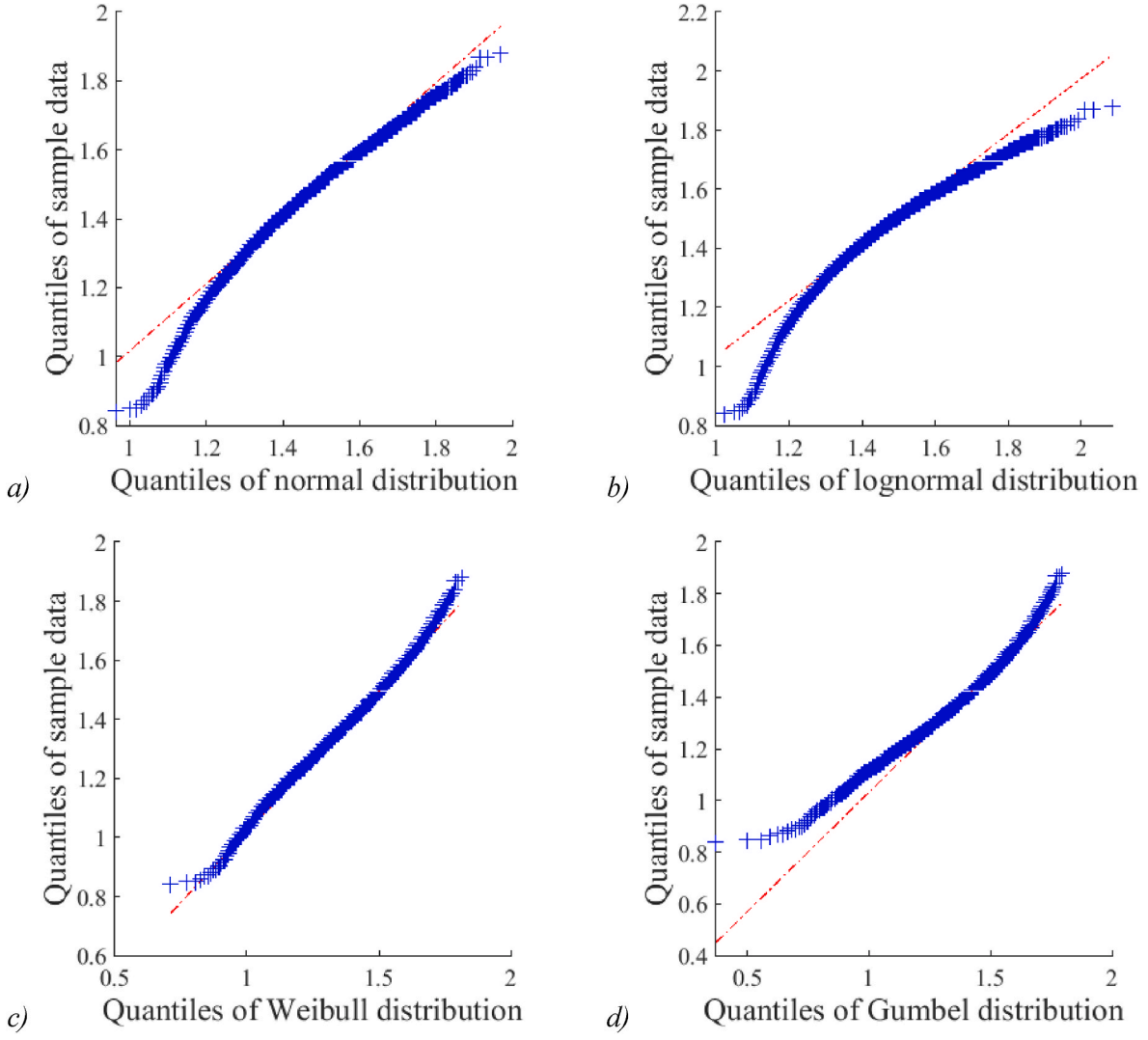

Fig. 25. Quantiles of sample data versus theoretical quantiles of a) normal, b) lognormal, c) Weibull, and d) Gumbel distributions.

Table 3
Results of the stochastic analysis.

Parameter	Simulation	Distribution			
		Normal	Lognormal	Weibull	Gumbel
Characteristic value α_c (5%)	1.236	1.256	1.259	1.216	1.185
Design value α_d (1‰)	0.906	1.071	1.104	0.901	0.781
P_f [%]	0.279	0.013	0.001	0.392	1.032
$P_s = 1 - P_f$ [%]	99.721	99.987	99.999	99.608	98.968
$\gamma_{M1} = \alpha_c/\alpha_d$	1.36	1.17	1.14	1.35	1.52

material parameters are taken into account with normal distributions; however, it is shown that reduced plate thickness due to corrosion governs the structural behaviour.

In addition, results of the stochastic analysis are summarized in Table 3. Characteristic and design load factors are determined for P_f = 5% and 1‰, respectively. Failure probability is also assessed for load factor equal to 1, which is equivalent to the condition of the performance function $g \leq 0$. The table includes survival probability $P_s = 1 - P_f$ as well since reliability index β cannot be used in the analysed case (applicable only for normal distributions). Based on the q-q plots, Weibull distribution fits sample data well, which is a non-normal distribution. Another important finding of the research is that design value could be evaluated in general by using the characteristic value and $\gamma_{M1} = 1.10$ for stability resistance according to EN 1993-1-5. However, it is shown that the ratio of characteristic and design values is 1.36 for the Monte Carlo simulation-based sample data, which highlights the significance of using different partial factors for considerably corroded steel elements. These results show the partial safety factor for the given case do not provide enough safety. Current results call the attention to the improvement of the partial safety factor for corroded members, that needs more investigations, measurements and calculations.

Data in the table are in accordance with the q-q plots. Weibull distribution gives the closest results to the simulation results. Survival probabilities show that normal and lognormal distributions are on the unsafe side regarding design theory and risk assessment, while Weibull and Gumbel distributions are on the safe side.

It can be stated that corrosion damage of steel plates governs the failure mode and ultimate load level. Thus, the best fitted probability function uses Weibull distribution, which is demonstrated by q-q plots, survival probabilities and evaluated partial factors as well. Based on the numerical simulation results the failure probability (P_f) is equal to $2.79 \cdot 10^{-3}$ which is significantly larger than the target value according to the EN 1990 regarding 1 year lifetime ($\beta = 4{,}7$; $P_f = 10^{-6}$). Therefore, the bridge deck can be verified only by the reduction of the loading side to keep the bridge in operation for one additional year. It is well-known that the dynamic amplification factor can be significantly smaller than the currently used design value ($\Phi = 1.4$), especially for bridges in downtown area with relatively small traffic loads. Therefore, reduction of the dynamic amplification factor could be made based on previous experiences or on-site measurements, which increases the survival probability.

8. Summary

Numerical model-based risk assessment and resistance calculation has been executed to evaluate the reliability and usability of the corroded deck system of the historical Széchenyi chain bridge. The paper introduced the applied risk assessment methodology, which contains the following key aspects: (i) corrosion grade evaluation based on on-site measurements, (ii) GMNI analysis-based resistance calculation using advanced numerical models, and (iii) FORM analysis using Monte Carlo simulations performing GMNIA calculations. The resistance of the bridge deck system has been determined by deterministic and stochastic methods. Their advantages, disadvantages, differences, and limitations are highlighted in the paper.

The presented novel resistance calculation method and risk assessment technique made it possible to keep the bridge for one additional year in operation until the refurbishment process could be prepared and started. The analysis and evaluation method are presented in the paper to demonstrate a powerful tool to analyse aging historical structures and serves as a case study and correct application for further investigations. It is also a demonstrative example to combine advanced finite element model-based design (direct resistance verification using GMNI analysis) and Monte Carlo analysis-based risk assessment. Based on the current investigations the following four main conclusions can be summarized:

- risk of failure is determined and specified for the governing optional failure mode for this particular structure,
- results of the stochastic analysis show that Weibull-type distribution fits sample data well,
- risk of failure and reliability index for the given lifetime period of corroded members should not be calculated based on normal (Gaussian) distribution,
- corrosion results in a highly unsymmetrical distribution, which should be considered in the risk assessment,
- survival probability P_s should be determined instead of the reliability index (β) for non-normally distributed performance function in the case of corroded members,
- by determining the characteristic and design values of the shear buckling resistance the applicability of the partial safety factor (γ_{M1} = 1.10) is questioned for corroded steel members since corrosion increases uncertainties of the resistance side.

Author statement

Balázs Kövesdi: Conceptualization, Methodology, Supervision, Writing – review & editing. **Dénes Kollár**: Software, Data curation, Investigation, Writing – original draft, Visualization. **László Dunai**: Conceptualization, Methodology, Supervision, Writing – review & editing. **Adrián Horváth**: Conceptualization, Methodology, Supervision, Writing – review & editing.

Declaration of competing interest

The authors declare that they have no known competing financial interests or personal relationships that could have appeared to influence the work reported in this paper.

Acknowledgement

The presented research program has been financially supported by the Grant MTA-BME Lendület LP2021-06/2021 “Theory of new generation steel bridges” program of the Hungarian Academy of Sciences. The research reported in this paper and carried out at the Budapest University of Technology and Economics has been supported by the National Research Development and Innovation Fund (TKP2020 Institution Excellence Subprogram, Grant No. BME-IE-WAT) based on the charter of bolster issued by the National Research Development and Innovation Office under the auspices of the Ministry for Innovation and Technology. Financial supports are gratefully acknowledged.

References

[1] Balázs Kövesdi, Péter Dunai, László Dunai, Structural analysis of the historical Széchenyi chain bridge in Budapest, in: Proceedings of the 8th European Conference on Steel and Composite Structures, Eurosteel, 2017, pp. 4049–4058, 2017.
[2] In-Tae Kim, Duy Kien Dao, Young-Soo Jeong, Jungwon Huh, Jin-Hee Ahn, Effect of corrosion on the tension behavior of painted structural steel members, J. Constr. Steel Res. 125 (2016) 205–217.

[3] Jeom Kee Paik, Do Kyun Kim, Advanced method for the development of an empirical model to predict time-dependent corrosion wastage, Corrosion Sci. 63 (2012) 51–58.
[4] G. Ruiz-Menéndez, C. Andrade, G. Carro-Sevillano, C. Peña, P. Adeva, J. Medina, R. Fernández, Identification of the failure mode of corroding steel rebars in a viaduct in service through hardness measurements, Results in Engineering 13 (100331) (2022) 12.
[5] Guang-chong Qin, Shan-hua Xu, Dao-qiang Yao, Zong-xing Zhang, Study on the degradation of mechanical properties of corroded steel plates based on surface topography, J. Constr. Steel Res. 125 (2016) 205–217.
[6] Yu-Chen Ou, Yudas Tadeus Teddy Susanto, Hwasung Roh, Tensile behavior of naturally and artificially corroded steel bars, Construct. Build. Mater. 103 (2016) 93–104.
[7] Sajjad Tohodi, Yasser Sharifi, Load-carrying capacity of locally corroded steel plate girder ends using artificial neural network, Thin-Walled Struct. 100 (2016) 48–61.
[8] Youde Wang, Shanhua Xu, Hao Wang, Anbang Li, Predicting the residual strength and deformability of corroded steel plate based on the corrosion morphology, Construct. Build. Mater. 152 (2017) 777–793.
[9] EN, Eurocode – Basis of Structural Design, 1990.
[10] Mahdi Shadabfar, Hongwei Huang, Hadi Kordestani, V. Edmond, Muho, Probabilistic modeling of excavation-induced damage depth around rock-excavated tunnels, Results in Engineering 5 (100075) (2020) 13.
[11] EN 1992-1-1, Eurocode 2: Design of Concrete Structures - Part 1-1: General Rules and Rules for Buildings.
[12] ÚT 2-3.402 (e-UT 07.02.11), Design of highway bridges: General rules, Hungarian Highway Association, 2004 (in Hungarian).
[13] EN 1993-1-5, Eurocode 3: Design of Steel Structures - Part 1-5: General Rules - Plated Structural Elements.
[14] EN 1993-1-1, Eurocode 3: Design of Steel Structures - Part 1-1: General Rules and Rules for Buildings.